JOURNAL OF NEUROSURGERY:
Case Lessons

J Neurosurg Case Lessons 3(23): CASE22100, 2022
DOI: 10.3171/CASE22100

Efficacy of intraarterial indocyanine green videoangiography in surgery for arteriovenous fistula at the craniocervical junction in a hybrid operating room: illustrative cases

Kenji Shimada, MD, PhD, Izumi Yamaguchi, MD, PhD, Takeshi Miyamoto, MD, PhD, Shu Sogabe, MD, PhD, Kazuhisa Miyake, MD, PhD, Yasuhisa Kanematsu, MD, PhD, and Yasushi Takagi, MD, PhD

Department of Neurosurgery, Tokushima University, Tokushima, Japan

BACKGROUND Sufficient understanding of the angioarchitecture of an arteriovenous fistula (AVF) at the craniocervical junction (CCJ) is crucial to surgical treatment but is often difficult because of the complex vascular anatomy. Intraarterial indocyanine green (ICG) videoangiography has emerged as a more useful option for understanding the vascular anatomy than intravenous ICG videoangiography. This report describes two cases of CCJ AVFs successfully treated by surgery using intraarterial ICG videoangiography and describes the efficacy of this technique.

OBSERVATIONS Case 1 involved a 71-year-old man presenting with tetraparesis after sudden onset of severe headache due to subarachnoid hemorrhage (SAH). Digital subtraction angiography (DSA) demonstrated CCJ epidural AVF. Intraarterial ICG videoangiography revealed the drainer, which had been difficult to identify. The AVF disappeared after disconnection of the drainer. Case 2 involved a 68-year-old man presenting with severe headache due to SAH. DSA showed multiple AVFs at the CCJ and cerebellar tentorium. Intraarterial ICG videoangiography demonstrated concomitant perimedullary AVF and dural AVF at the CCJ. All AVFs disappeared postoperatively.

LESSONS Intraarterial ICG videoangiography was useful for definitive diagnosis of CCJ AVF, facilitating identification of feeders and drainers with bright and high phase contrast and allowing repeated testing to confirm flow direction.

https://thejns.org/doi/abs/10.3171/CASE22100

KEYWORDS craniocervical junction; arteriovenous fistula; intraarterial ICG videoangiography; feeder; drainer

Arteriovenous fistula (AVF) at the craniocervical junction (CCJ) is typically treated surgically rather than by endovascular treatment. Recently, neurosurgery has been reported to result in better treatment outcomes than endovascular treatment.[1] A sufficient understanding of the angioarchitecture and accurate diagnosis of CCJ AVF is crucial for safe and complete surgical elimination but is often difficult due to the complex angioarchitecture of this lesion despite recent advances in angiography.

Indocyanine green (ICG) videoangiography is frequently used in vascular neurosurgery because of the integration of equipment for this modality into operative microscopes. However, in cases of intravenous ICG videoangiography, ICG remains in the vessels during the late phase, presenting an obstacle to understanding the vascular anatomy. In addition, because of the large amount of ICG required to reach the intracranial arteries due to dilution in the cardiopulmonary circulation, a long washout time is required to remove the ICG. Intraarterial ICG videoangiography was recently found to be more useful for vascular neurosurgery by overcoming these technical limitations of intravenous ICG videoangiography.[2,3] We previously reported the usefulness of intraarterial ICG videoangiography for arteriovenous malformation and hemangioblastoma surgery.[4,5] This technique helps surgeons understand the angioarchitecture of vascular malformation more easily than with intravenous ICG videoangiography because of brighter and higher phase contrast. Further, the method is easily repeated due to the short ICG washout time, unlike intravenous ICG videoangiography.[4,5] Here, we present two cases of CCJ AVFs in which intraarterial ICG

ABBREVIATIONS AVF = arteriovenous fistula; CCJ = craniocervical junction; CT = computed tomography; DSA = digital subtraction angiography; ICG = indocyanine green; MIP = maximum intensity projection; SAH = subarachnoid hemorrhage; TAE = transarterial embolization; VA = vertebral artery; 3DRA = three-dimensional rotational angiography.

INCLUDE WHEN CITING Published June 6, 2022; DOI: 10.3171/CASE22100.
SUBMITTED March 2, 2022. **ACCEPTED** March 23, 2022.

© 2022 The authors, CC BY-NC-ND 4.0 (http://creativecommons.org/licenses/by-nc-nd/4.0/).

videoangiography proved useful for accurate diagnosis and successful treatment. Intraarterial ICG videoangiography was approved by the ethics review board at Tokushima University.

Illustrative Cases

Case 1

A 71-year-old man presented with tetraparesis after sudden onset of severe headache. Computed tomography (CT) revealed a subarachnoid hemorrhage (SAH), mainly in the prepontine and premedullary cistern (Fig. 1A). Digital subtraction angiography (DSA) demonstrated a CCJ epidural AVF at the right C1–2 level (Fig. 1B). The fistula was mainly fed by the right C2 segmental artery and drained into the epidural venous plexus (Fig. 1B). The epidural drainage route was the subcutaneous cavernous sinus and posterior cervical vein (Fig. 1B). The intradural drainage route was the radicular vein leading to the anterior medullary vein, which was thought to be the cause of SAH (Fig. 1B). Slab maximum intensity projection (MIP) images revealed that the intradural drainage route originated from the ventral epidural venous plexus and ran along the ventral root of the right C2 nerve (Fig. 1C). The patient received emergency endovascular transarterial embolization (TAE) to reduce shunt flow and prevent rebleeding. A microcatheter was introduced into the right C2 segmental artery, and feeder occlusion was performed by coil embolization. Although shunt flow significantly reduced after TAE (Fig. 1D), DSA after 2 weeks showed AVF recurrence and varix on the intradural drainage route, which was estimated to represent the source of bleeding (Fig. 1E). Surgical interruption of the intradural draining vein was therefore performed in a hybrid operating room. One day before surgery, coil embolization of the epidural venous plexus was performed with the aim of reducing the volume of intraoperative bleeding (Fig. 1F).

After inducing general anesthesia, the patient was positioned prone. A 4-Fr sheath was inserted into the right radial artery. A heparin-coated 4-Fr catheter was then introduced into the right vertebral artery (VA). Right C1 and C2 hemilaminectomies were then performed. After opening the dura mater and cutting the dorsal root of the right C2 nerve and dentate ligament, identifying the drainer proved difficult (Fig. 2A). Intraarterial ICG videoangiography was therefore performed by injecting ICG through the catheter placed in the right VA using an ICG videoangiography technology-integrated microscope (Kinevo 900, Carl Zeiss). ICG videoangiography revealed a drainer appearing at 1 second (Fig. 2B), after which normal vessels appeared at 4 seconds (Fig. 2C). However, the varix could not be identified by intraarterial ICG videoangiography. Intraoperative DSA was therefore performed to confirm whether the varix was on the distal part of the drainer. A clip was placed next to the drainer as a landmark (Fig. 2D). Intraoperative DSA showed that the drainer descended and turned around near the clip and then ascended (Fig. 2E). Varix was confirmed on the drainer just medial to the clip (Fig. 2E). The drainer was disconnected (Fig. 2F), and

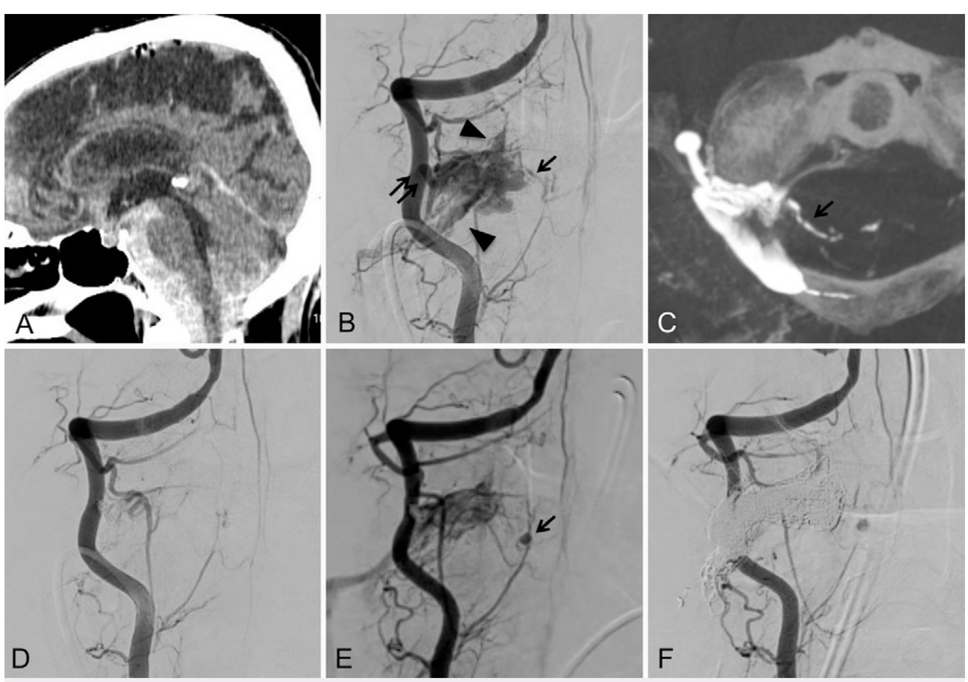

FIG. 1. Case 1. **A:** Sagittal CT shows SAH in the prepontine and premedullary cisterns. **B:** Anteroposterior (AP) right vertebral angiography (VAG) demonstrated an epidural AVF of the craniocervical junction at the right C1–2 level. The fistula was mainly fed by the C2 segmental artery (*double arrows*) and drained into the epidural venous plexus. The epidural drainage route was the subcutaneous cavernous sinus and posterior cervical vein (*arrowheads*). The intradural drainage route was the radicular vein (*single arrow*) leading to the anterior medullary vein. **C:** Slab MIP image reveals the intradural drainage route (*arrow*) originating from the ventral epidural venous plexus and running along the ventral root of the right C2 nerve. **D:** Right VAG, AP view, showed significantly reduced shunt flow after coil embolization of the feeder from the right C2 segmental artery. **E:** Right VAG, AP view, after 2 weeks revealed AVF recurrence and varix (*arrow*) on the intradural drainage route. **F:** Right VAG, AP view, showed coil embolization of the epidural venous plexus.

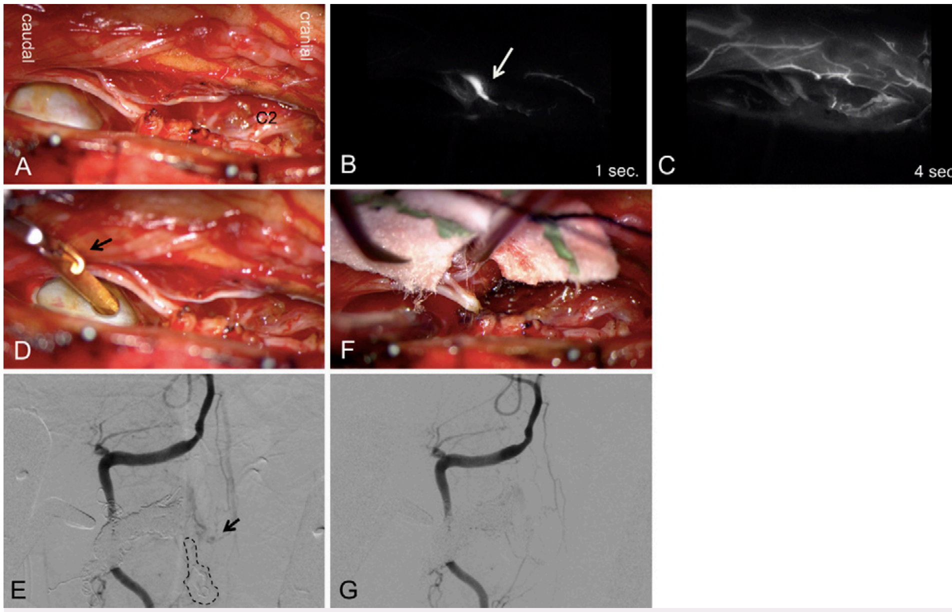

FIG. 2. Case 1. Intraoperative view (**A**) and intraarterial ICG videoangiography studies (**B and C**) before disconnection of the drainer. ICG videoangiography revealed a drainer (*arrow*) appearing at 1 second (**B**), after which normal vessels appeared at 4 seconds (**C**). Intraoperative view demonstrates a clip (*arrow*) placed next to the drainer as a landmark (**D**). Intraoperative DSA (**E**) showed the drainer descending, turning around near the clip (*dotted area*), and ascending, and a varix (*arrow*) was confirmed to be on the drainer just medial to the clip. Intraoperative view shows the drainer is disconnected (**F**), and intraoperative DSA demonstrated complete disappearance of the shunt (**G**).

intraoperative DSA demonstrated complete disappearance of the shunt (Fig. 2G). Symptoms improved postoperatively, and the patient was transferred to the rehabilitation hospital.

Case 2

A 68-year-old man presented with severe headache. CT revealed SAH in the right cerebellomedullary cistern (Fig. 3A). DSA showed CCJ AVF at the C1 level and tentorial dural AVF (Fig. 3B). The CCJ AVF was mainly fed by the C1 segmental artery and drained into the medullary vein (Fig. 3B). The tentorial dural AVF was fed by the posterior meningeal artery and drained into the inferior vermian vein (Fig. 3B). CCJ AVF was estimated to be the cause of SAH from the distribution of hemorrhage. Subsequent three-dimensional rotational angiography (3DRA) revealed that the CCJ AVF was fed by the radiculopial artery from the right C1 segmental artery, which ran laterally and then turned medial and inferoposterior and drained into the medullary vein (Fig. 3C). The caliber change between the feeder and drainer apparent on 3DRA (Fig. 3D), which was indicated as a fistulous point, seemed to be on the lateral surface of the medulla as demonstrated by slab MIP images (Fig. 3E). However, slab MIP images also showed radicular veins connected to the medullary vein and tangled with the right C1 nerve (Fig. 3E). The fistulous points seemed to be located at two different points, one on the lateral surface of the medulla and the other on the dura or C1 nerve root, suggesting concomitant perimedullary AVF and dural or radicular AVF as well as tentorial dural AVF. Preoperative neuroradiological examinations alone were insufficient for revealing definitive diagnoses. The patient underwent interruption of draining veins for both the CCJ AVF and tentorial dural AVF in the hybrid operating room.

After receiving general anesthesia, the patient was positioned prone. A 4-Fr sheath was inserted into the right radial artery. A heparin-coated 4-Fr catheter was then introduced into the right VA. Midline suboccipital craniotomy and C1 laminectomy were then performed. After opening the dura mater and cutting the dentate ligament, a feeder from the radiculopial artery and drainers on the ventral root of the right C1 nerve were identified (Fig. 4A). Intraarterial ICG videoangiography revealed that the feeder from the radiculopial artery, the fistulous point on the lateral surface of the medulla and drainers on the medullary side and dural side, appeared at 0.5 seconds (Fig. 4B), after which the ICG appearance of drainers on both sides increased at 1 second (Fig. 4C), with both connecting at 1.5 seconds (Fig. 4D). The fistulous point on the lateral surface of the medulla was dissected and coagulated (Fig. 4E). After that, intraarterial ICG videoangiography demonstrated the shunt flow direction more clearly, with the drainer flowing from the dural side to the medullary side on the C1 nerve root (Fig. 4F–H), suggesting remnant dural AVF. The draining vein was therefore disconnected with the ventral root of the right C1 nerve (Fig. 4I). Intraarterial ICG videoangiography showed complete elimination of the CCJ AVFs (Fig. 4J). The dural opening was extended superiorly to expose the inferior vermian vein as the drainer of the tentorial dural AVF. This drainer was disconnected at the site of entry into the intracranial space. Intraoperatively and 2 weeks postoperatively, DSA showed that all AVFs had completely disappeared (Fig. 3F). The postoperative course was uneventful, and the patient was discharged without any neurological deficits.

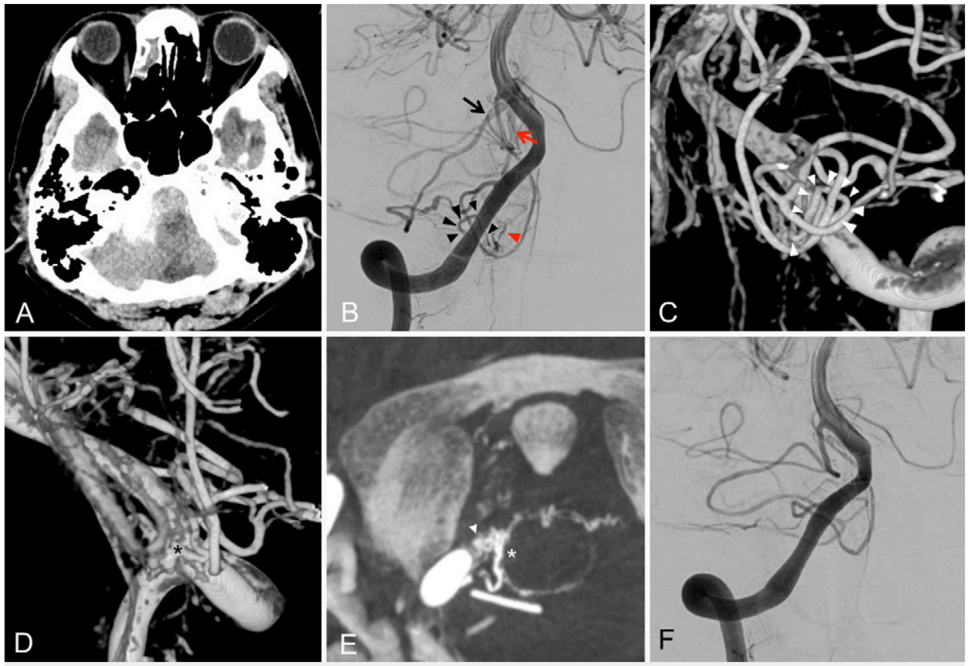

FIG. 3. Case 2. **A:** CT reveals SAH in the right cerebellomedullary cistern. **B:** Right VAG, AP view, showed CCJ AVF at the C1 level and a tentorial dural AVF. The CCJ AVF was mainly fed by the C1 segmental artery (*black arrowheads*) and drained to the medullary vein (*red arrowhead*). The tentorial dural AVF was fed by the posterior meningeal artery (*black arrow*) and drained to the inferior vermian vein (*red arrow*). **C:** On 3DRA, a CCJ AVF was seen to be fed by a radiculopial artery from the right C1 segmental artery, which ran laterally and then turned medially and inferoposteriorly (arrowheads) and drained into the medullary vein. D: Further 3DRA demonstrated caliber change (*asterisk*) between the feeder and drainer, which was indicated as the fistulous point. **E:** Slab MIP image shows that the fistulous point (*asterisk*) seems to be on the lateral surface of the medulla. The slab MIP image also shows radicular veins (*arrowhead*) connecting to the medullary vein and tangled with the right C1 nerve. **F:** Right VAG, AP view, at 2 weeks postoperatively showed that all AVFs had completely disappeared.

Discussion

This report demonstrated that intraarterial ICG videoangiography as well as intraoperative DSA were helpful for understanding the angioarchitecture and reaching a definitive diagnosis in CCJ AVF surgery. In Case 1, intraarterial ICG videoangiography clearly revealed the drainer that had been difficult to recognize in the surgical field, and intraoperative DSA showed a varix that had not been apparent in the surgical field along the draining route. In Case 2, frame-by-frame review of intraarterial ICG videoangiography with bright and high-phase contrast helped identify feeders and drainers and clarify shunt flow direction. Intraarterial ICG videoangiography after coagulating a fistulous point on the lateral surface of the medulla demonstrated the remaining dural AVF more clearly compared to that before coagulating the fistulous point by showing the direction of drainage flow from the dural side to the medullary side. Repeated videoangiography thus allowed quick comparison of multiple studies due to the short span and easy recognition of flow direction. This crucial information obtained by intraoperative DSA and intraarterial ICG videoangiography contributed to safe, effective, and complete obliteration of the CCJ AVF. In addition, as compared to intravenous ICG videoangiography, intraarterial ICG videoangiography is not time-consuming because it can be also performed with intraoperative DSA, which is an indispensable procedure for vascular malformation surgery in the hybrid operating room.

Recent reports have demonstrated that intraarterial injection of ICG results in better contrast and a shorter ICG clearance time as compared to intravenous injection because intravenously injected ICG remains in the vessels for approximately 15 minutes, whereas only 1 minute is needed to clear intraarterially injected ICG.[2–4] This happens because 2.5 mg/mL of ICG is usually injected for intravenous use, whereas a much lower dose (0.05 mg/mL in our cases) is used for intraarterial injection. Bright, high-phase contrast and the repeatability of intraarterial ICG videoangiography facilitated easy recognition of feeders and drainers as well as shunt flow direction, all of which are requisite for the accurate diagnosis of CCJ AVF with a complex angioarchitecture. The efficacy of intraarterial fluorescence videoangiography in CCJ AVF surgery has been reported, with frame-by-frame review of fluorescence videoangiography reported as useful for identifying the accurate anatomy of CCJ AVF.[6] In the present study, we demonstrated for the first time that intraarterial ICG videoangiography is also useful for CCJ AVF surgery.

A key disadvantage of intraarterial ICG videoangiography is that it cannot detect feeders or drainers behind the spinal cord. All feeding and draining vessels can be visualized by intraoperative DSA but not by ICG videoangiography. In Case 1 of the present report, although intraarterial ICG videoangiography did not reveal any varix behind the spinal cord, the varix was confirmed along the route of the drainer by intraoperative DSA. Therefore, unlike bypass or

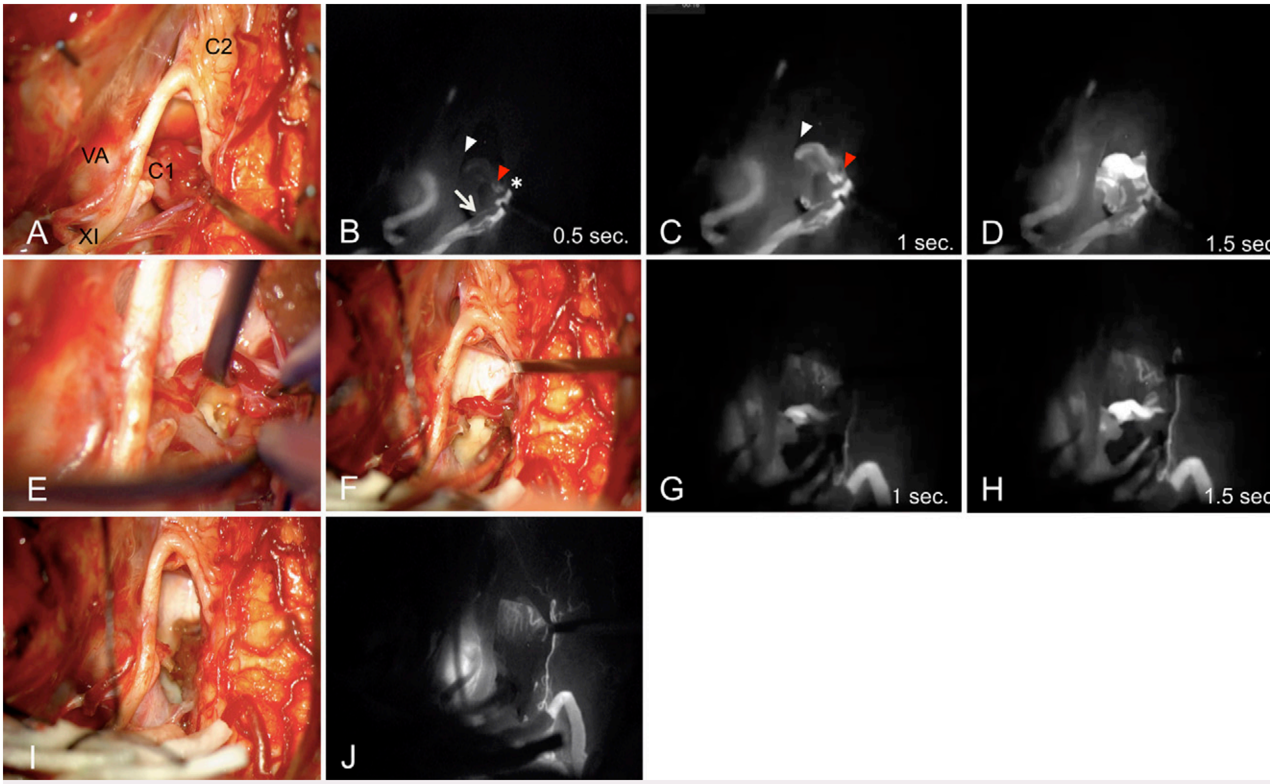

FIG. 4. Case 2. Surgical views before coagulating the fistulous point of the perimedullary AVF (**A**), while coagulating the fistulous point of the perimedullary AVF (**E**), after coagulating the fistulous point of the perimedullary AVF (**F**), and after disconnecting the drainer of the dural AVF (**I**), and ICG videoangiography studies before coagulating the fistulous point (**B to D**), after coagulating the fistulous point (**G and H**), and after disconnecting the drainer of the dural AVF (**J**). Intraarterial ICG videoangiography revealed a feeder from the radiculopial artery (**B**, *arrow*), the fistulous point on the lateral surface of the medulla (**B**, *asterisk*), and drainers of the medullary side (*red arrowhead*) and dural side (*white arrowhead*) appearing at 0.5 seconds. ICG appearance of drainers on both sides increased at 1 second (**C**, *red and white arrowheads*), and then both connected at 1.5 seconds (**D**). Intraarterial ICG videoangiography demonstrated shunt flow direction more clearly, with the drainer appearing from the dural side at 1 second (**G**) and then the medullary side at 1.5 seconds (**H**), indicating the drainer flowing from the dural side to medullary side. Intraarterial ICG videoangiography showed complete elimination of the AVFs (**J**).

aneurysm surgery, routine intraoperative DSA is indispensable in our institution for vascular malformation surgery to compensate for ICG videoangiography. However, intraoperative DSA is inferior to intraarterial ICG videoangiography with regard to the simplicity, speed, and spatial resolution of the surgical view because ICG videoangiography can detect vessels in the same plane as the operative microscopic view. Thus, the operator can easily and rapidly detect feeders and drainers without disturbing the surgical procedure. We have therefore now added the step of injecting ICG into the contrast medium administered through the catheter. Intraarterial ICG videoangiography and intraoperative DSA therefore compensate for each other's disadvantages. Although introducing a catheter is time-consuming and carries some risk of thromboembolic complications, inserting a catheter into the VA via the radial artery is not particularly difficult with the patient in a prone position. We have not encountered any adverse coagulation events in our institute, thanks to the implementation of countermeasures involving mandatory connection of all catheters to a pressurized heparinized saline bag for the purpose of flushing, with catheter irrigation performed every 15 minutes.[4,5]

Some studies have reported concomitant dural and perimedullary AVFs at the CCJ, with a cooccurrence rate of 38% to 43%.[6–8] Recent developments in various neuroradiological modalities and accumulation of surgical experience have led to the identification of radicular AVF on the spinal nerves located between the spinal cord and dura in which radiculomeningeal and pial feeders connect with the radicular vein at the same fistulous point.[9,10] In Case 2 of our report, radicular AVF was ruled out based on the lack of a fistulous point or feeders from the radiculomeningeal artery on the nerve root demonstrated by intraarterial ICG videoangiography. Hiramatsu et al. classified CCJ AVF into five subgroups.[11] According to that classification, Case 1 was designated as Type 4 (epidural AVF) and Case 2 as cooccurrence of Type 1 (dural AVF) and Type 5 (perimedullary AVF). Meticulous preoperative angiographic investigation, including slab MIP images as well as repeated intraarterial ICG videoangiography with bright and high-phase contrast, is critical for accurate diagnosis and safe treatment of CCJ AVF.

Observations

We have reported for the first time two cases of CCJ AVFs that were successfully treated using intraarterial ICG videoangiography.

Lessons

Intraarterial ICG videoangiography was useful for definitive diagnosis, allowing easy identification of feeders and drainers with bright and high-phase contrast and repeated performance to confirm flow direction.

References

1. Takai K, Endo T, Seki T, Inoue T, Koyanagi I, Mitsuhara T. Neurosurgical versus endovascular treatment of craniocervical junction arteriovenous fistulas: a multicenter cohort study of 97 patients. *J Neurosurg.* Published online December 31, 2021. doi: 10.3171/2021.10.JNS212205.
2. Horie N, So G, Debata A, et al. Intra-arterial indocyanine green angiography in the management of spinal arteriovenous fistulae: technical case reports. *Spine (Phila Pa 1976).* 2012;37(4):E264–E267.
3. Yoshioka H, Kinouchi H, Nishiyama Y, et al. Advantage of microscope integrated for both indocyanine green and fluorescein videoangiography on aneurysmal surgery: case report. *Neurol Med Chir (Tokyo).* 2014;54(3):192–195.
4. Shimada K, Yamaguchi T, Miyamoto T, et al. Efficacy of intraarterial superselective indocyanine green videoangiography in cerebral arteriovenous malformation surgery in a hybrid operating room. *J Neurosurg.* 2020;134(5):1544–1552.
5. Shimada K, Yamamoto Y, Miyamoto T, et al. Efficacy of intra-arterial indocyanine green videoangiography in hemangioblastoma surgery: a case report. *NMC Case Rep J.* 2021;8(1):295–300.
6. Kanemaru K, Yoshioka H, Hashimoto K, et al. Efficacy of intraarterial fluorescence video angiography in surgery for dural and perimedullary arteriovenous fistula at craniocervical junction. *World Neurosurg.* 2019;126:e573–e579.
7. Sato H, Wada H, Noro S, Saga T, Kamada K. Subarachnoid hemorrhage with concurrent dural and perimedullary arteriovenous fistulas at craniocervical junction: case report and literature review. *World Neurosurg.* 2019;127:331–334.
8. Sato K, Endo T, Niizuma K, et al. Concurrent dural and perimedullary arteriovenous fistulas at the craniocervical junction: case series with special reference to angioarchitecture. *J Neurosurg.* 2013;118(2):451–459.
9. Takai K, Komori T, Kurita H, Kawai K, Inoue T, Taniguchi M. Intradural radicular arteriovenous fistula that mimics dural arteriovenous fistula: report of three cases. *Neuroradiology.* 2019;61(10):1203–1208.
10. Matsubara S, Toi H, Takai H, et al. Variations and management for patients with craniocervical junction arteriovenous fistulas: comparison of dural, radicular, and epidural arteriovenous fistulas. *Surg Neurol Int.* 2021;12:411.
11. Hiramatsu M, Sugiu K, Ishiguro T, et al. Angioarchitecture of arteriovenous fistulas at the craniocervical junction: a multicenter cohort study of 54 patients. *J Neurosurg.* 2018;128(6):1839–1849.

Disclosures

The authors report no conflict of interest concerning the materials or methods used in this study or the findings specified in this paper.

Author Contributions

Conception and design: Shimada, Kanematsu, Takagi. Acquisition of data: all authors. Analysis and interpretation of data: Shimada, Miyake, Kanematsu. Drafting the article: Shimada. Critically revising the article: Shimada, Kanematsu. Reviewed submitted version of manuscript: Shimada, Kanematsu, Takagi. Approved the final version of the manuscript on behalf of all authors: Shimada. Statistical analysis: Shimada. Administrative/technical/material support: Shimada. Study supervision: Shimada, Takagi.

Correspondence

Kenji Shimada: Tokushima University, Tokushima, Japan. s_kenji1032@yahoo.co.jp.